frontiers | Frontiers in Marine Science

TYPE Original Research
PUBLISHED 21 November 2024
DOI 10.3389/fmars.2024.1198106

OPEN ACCESS

EDITED BY
Matthieu Le Hénaff,
Atlantic Oceanographic and Meteorological Laboratory (NOAA), United States

REVIEWED BY
Agus Setiawan,
National Research and Innovation Agency, Indonesia
Elisabete De Santis Braga,
University of São Paulo, Brazil

*CORRESPONDENCE
Kanga Désiré Kouame
kangadesirek@gmail.com

RECEIVED 31 March 2023
ACCEPTED 28 October 2024
PUBLISHED 21 November 2024

CITATION
Kouame KD, N'Guessan KB, Kouassi AM, Trokourey A, Ostrowski M and Brehmer P (2024) Unravelling nutrient dynamics and mixed layer depth variability in the equatorial Atlantic: insights from 10°W meridional section monitoring.
Front. Mar. Sci. 11:1198106.
doi: 10.3389/fmars.2024.1198106

Unravelling nutrient dynamics and mixed layer depth variability in the equatorial Atlantic: insights from 10°W meridional section monitoring

Kanga Désiré Kouame[1,2]*, Kouadio Benjamin N'Guessan[1,2], Aka Marcel Kouassi[1], Albert Trokourey[2], Marek Ostrowski[3] and Patrice Brehmer[4]

[1]Département Environnement, Centre de Recherches Océanologiques (CRO), Abidjan, Côte d'Ivoire, [2]Laboratory of Constitution and Reaction of Matter, Université Félix Houphouët Boigny (UFHB), Abidjan, Côte d'Ivoire, [3]Institute of Marine Research and Bjerknes Centre for Climate Research, Bergen, Norway, [4]IRD, Univ Brest, CNRS, Ifremer, Lemar, Commission Sous Régionale des Pêches (CSRP), Sub-Regional Fisheries Commission (SRFC), Dakar, Senegal

The ocean, a pivotal component of the Earth's climate system, exerts a profound global influence through intricate physical and biological interactions within its surface layer. This interplay centers around the mixed layer (ML), integral for energy exchange driven by oceanic currents. An essential regulatory function of the ocean involves orchestrating the distribution of chemical elements, with nitrate assuming a pivotal role in oceanic primary production. Nutrient availability, a cornerstone of primary production, hinges on the mixed layer depth (MLD) dynamics, modulated by many mechanisms, including upwelling and convection. This study unravels the interplay between nutrient variability and MLD depth, focusing on the Gulf of Guinea (GG) region in the equatorial Atlantic. Characterization of the study area reveals distinctive sea surface temperature (SST), salinity (SSS), and current patterns. The South Equatorial Undercurrent (SEUC) and Equatorial Undercurrent (EUC) play vital roles in surface nutrient transport. Nitrate distribution unveils latitudinal variations, exhibiting pronounced enrichment during boreal summer and winter. The equatorial region experiences a strengthening of MLDs from 10.5 to 35.33 m in summer, which increases the nitrate input from 0 to 2.06 mmol m^{-3} in the surface layers in the mixed layer. In contrast, boreal winters experience more intense MLDs that vary between 20.5 and 64.50 m, supporting high nitrate concentrations of 2.96 to 7.49 mmol m^{-3}, challenging previous hypotheses. This equatorial enrichment is supported by low nitracline ranging from 5.47 to 46.19 m. Beyond the equator, the subequatorial and subtropical regions, despite the observed deepening of the ML, present low nitrate concentrations (less than 0.5 mmol m^{-3}) with a nitracline that does not reach the ML. However, at 6°S and 9°S, a respective increase in nitrate content of 0.66 mmol m^{-3} and 1.2 mmol m^{-3} influenced by internal waves, advection and

surface currents is observed. Temperature, salinity, and atmospheric fluxes shape nutrient distribution and primary production dynamics. These findings illuminate the intricate relationships between oceanographic processes, nutrient availability, and marine ecosystem productivity. A holistic understanding is crucial for sustainable resource management and fisheries in the equatorial Atlantic and beyond.

KEYWORDS

mixed layer, nitracline, nitrate concentration, upwelling, equatorial region, subequatorial region, subtropical region

1 Introduction

The ocean serves as a vital cog in the intricate machinery of the Earth's climate system, exerting a profound influence globally that reverberates. This influence hinges upon the interplay of physical and biological processes within the ocean's surface layer (Gruber et al., 2002). The mixed layer (ML) is central to this interaction, an essential conduit for exchanging energy driven by oceanic currents (Alvain, 2005).

A cornerstone of the ocean's regulatory function lies in its capacity to act as a reservoir, sink, and source for various chemical elements, thereby orchestrating their distribution within the water column. Among these elements, nitrate is crucial due to its central role in ocean primary production (Lévy et al., 2012; Morelle, 2017; Trombetta, 2019). Governed by nutrient availability, this primary production intricately hinges upon the dynamics of the mixed layer depth (MLD), a phenomenon underscored by seminal works such as Voituriez et al. (1982) and Wilson and Coles (2005). Nutrients, serving as crucial building blocks, are infused into the oceanic system through a multifaceted interplay of mechanisms, encompassing turbulence, internal waves, convection, diffusion, and, notably, upwelling (Mahadevan, 2016; McGillicuddy, 2016; Sylla, 2019; Ismail and Al Shehhi, 2022); (Brandt et al., 2023, 2024).

In this context, the variability of MLD emerges as a linchpin, exerting decisive control over the redistribution of nutrients throughout the water column and thereby shaping their accessibility to phytoplankton communities (Pershing, 2006). Particularly in temperate seas, the ebb and flow of MLD during different seasons emerge as a primary conduit for nutrient injection into the ocean surface layer, as demonstrated by D'Ortenzio et al. (2014).

Diverse methodologies are being used to unravel the nutrient availability dynamics within the ocean's surface layers. Some studies advocate for employing gradient intervals, where the steepest nutrient gradients materialize (Hales et al., 2005). Alternatively, proponents of other approaches champion the utilization of the ML's base (Schafstall et al., 2010) or isopycnal layers, as posited by Williams et al. (2006) and Aksnes et al. (2007).

While the Gulf of Guinea (GG) has attracted scholarly attention, elucidating the primary productivity and nutritional regime of the equatorial Atlantic (Voituriez and Herbland, 1979, 1981; Herbland et al., 1985; Le Bouteiller, 1986), studies delving into the intricate nexus between nutrient variability and MLD remain scarce. Notably, works such as Monger et al. (1997); Murtugudde et al. (1999); Nubi et al. (2019), and Radenac et al. (2020) offer glimpses into the complex tapestry of equatorial upwelling and its ramifications on bio-productivity and nitrate dynamics. However, a comprehensive investigation into the interplay between nutrient concentrations and MLD variation remains an uncharted frontier.

This study undertakes a pioneering quest to unravel the ramifications of MLD variations on the seasonal supply of nitrate, spanning the breadth from deep to surface layers along the meridional section at 10°W. By deciphering this intricate relationship, we aspire to fortify our ability to predict the response of oceanic ecosystems to the profound perturbations induced by climate change in the tropical Atlantic.

2 Material

2.1 Study area, data collection and processing

This study was conducted at 10°W between 2°N and 10°S (Figure 1) in the GG defined as the region extending from 15°S to 5°N and from 15°W to 15°E (Kolodziejczyk et al., 2014). The hydrological and nitrate data used were extracted from a box centered at 10°W ± 0.25° between latitudes 2°N and 10°S.

2.2 Hydrological data

These data consisted of historical and recent low and high-resolution CTD data with uneven spatial and temporal distributions, collected between October 1973 and March 2017 during several campaigns and programs. They come from the database of the EGEE program in close connection with PIRATA (Bourlès et al., 2007) and relate specifically to the GG through the research section of the African Monsoon Multidisciplinary Analysis (AMMA) program,

see http://www.amma-international.org). They were supplemented by data from CORIOLIS (http://www.CORIOLIS.eu.org/) and the Scientific Information System for the Sea (SISMER) of IFREMER.

2.3 Nitrate data

The data covers the period from October 1973 to September 2007 in an irregular time and space. We used the data from the first 100 meters of the water column for the present study. This allowed us to have 136 nitrate profiles.

Nitrates were measured on samples taken at 12 different depths between 0 and 150 m with the rosette associated with the probe. For the Sismer and Coriolis data, the analyses were carried out immediately on board with a Technicon auto-analyzer (Voituriez, 1983). Nitrate was measured on an Autoanalyzer II Technicon (Bran et Luebbe) following the standard method of Wood et al. (1967) described in the Manual of Tréguer and Le Corre (1975). Nitrate was reduced to nitrite, using a column of coppered cadmium and determined colourimetrically after diazotization with sulfanilamide and coupling with naphthyl-ethylene diamine following the technique of Bendschneider and Robinson (1952). Duplicate analyses of individual samples were performed repeatedly to estimate analytical error. This study focuses mainly on analyses in the equatorial region (2°N - 2°S) for both seasons and in the subequatorial (5°S-7°S) and subtropical (8°S-10°S) regions where the data were only available in the boreal summer. Emphasis is placed on depths between 0 and 100 m where biological activity is predominant (Nubi et al., 2016). For more details on sampling, quality control, and justification of the methodology, refer to Kouamé (2022).

3 Methods

3.1 Hydrological characteristics of the study area

To study the characteristics of this area, data were organized into the boreal winter (November to April) and the boreal summer (May to October). The averages of temperature and salinity between October 1973 and March 2017 and nitrate from October to November 2007 were calculated. Matlab script was used to produce temperature, salinity, and nitrate sections where data were available. The depth of the thermocline was represented by the D20 and shown on the salinity sections (Supplementary Figure S2) as a pink line. The Matlab contour function represents the contour lines on a 2D graph, with a colour gradient associated with the different intervals of corresponding temperature, salinity, and nitrate values. This allows to specify the number of lines to be plotted and specific values to be displayed.

3.2 Determining the depth of the mixed layer

The MLD was determined from individual profiles using the density threshold method of Holte and Talley (2009) with a criterion of 0.03 kg m^{-3} as performed by N'Guessan et al. (2020) and Kouamé (2022). Mean climatological MLDs were calculated for a 1-degree resolution grid between 2°N and 10°S. Latitudinal and monthly variability was obtained by representing the mean climatological MLD in a month-latitude Hovmöller diagram.

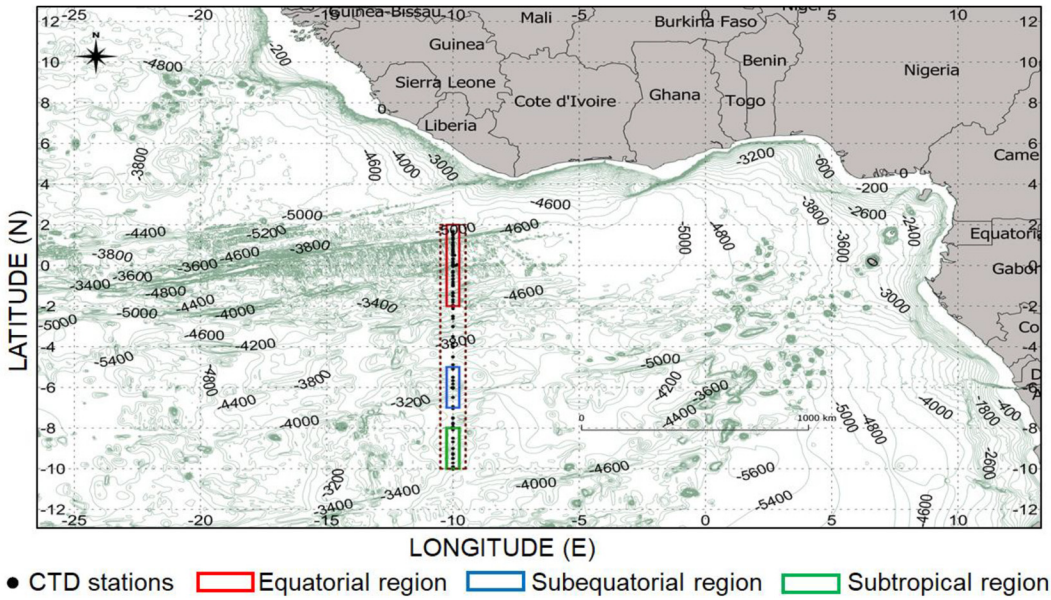

FIGURE 1
Maps of the Gulf of Guinea in the tropical Atlantic. Water depths are indicated in shades of color. The study area (red, blue and green boxes) at 10°W between 2°N-10°S derived from Sismer and Coriolis data. Black dots represent the vertical nitrate profile in the three regions and CTD sampling stations in the top 100 meters of the water column from October 1973 to November 2017 at 10°W. Numbers from 0 to 5000 represent isobaths.

3.3 Determination of the top of the nitracline and corresponding nitrate values

The top of the nitracline is determined for each nitrate profile. The centred and reduced variables produce a nitrate-density graph for each season. According to Hemsley (2016), using the same nitrate-density relationship can have limitations, as the nitrate-density relationship can vary by season and geographical area due to diapycnal mixing (Hummels et al., 2014).

The density intervals that best correspond to a zone of linearity are used to determine the polynomial that best fits the point cloud obtained, as performed by Hemsley (2016). Matlab's polyfit and polyval functions were used for this purpose, along with the LAR (Least Absolute Residuals) module, to minimize the absolute difference of residuals arising from the effect of the point cloud away from the fit. The polynomials obtained for each season and zone are then used to recalculate the concentration values on the nitrate profiles with a vertical resolution of 1 meter after linear interpolation. Negative concentrations obtained during this calculation are then replaced by zero.

Aksnes et al. (2007) determined the top of the nitracline from a threshold concentration of 1 mmol m^{-3} chosen based on nitrate sections (Supplementary Figure S3). This choice of a threshold of 1 mmol m^{-3} (the most significant value) of nitrate has been accepted by several authors (Oudot, 1983) as a criterion for enriching surface layers. Voituriez and Herbland (1984) had already used this threshold in the Eastern Equatorial Atlantic when studying the nitrate-temperature relationship in the equatorial upwelling of the GG. This threshold of 1 mmol m^{-3} was also used by Lavigne et al. (2013) in the Mediterranean Sea to study the control of MLD on phytoplankton phenology.

3.4 Calculation of nitrate concentration in the mixed layer

The stations containing nitrate data were used to determine the MLD on each profile based on the method selected following the graphical and statistical analysis. One hundred eight stations are used in the equatorial region, including 90 for the boreal summer and 18 for the boreal winter. South of the equator, 21 stations for the subequatorial region and 18 stations for the subtropical region are used in this study. Recalculated nitrate profiles determine nitrate concentrations in the layer by averaging the concentrations along the profile between the surface and the MLD value determined.

3.5 Study of variations in MLD, nitracline peak and nitrate distribution in the ocean surface layer

The average MLD, nitracline, and surface nitrate concentration in each area are calculated from the different profiles with a spatial resolution of 0.5-degree latitude between 2°N and 2°S and 0.25-degree latitude in the subequatorial and subtropical regions on the 10°W radial. These three parameters were plotted on a two-dimensional (2D) diagram with depth versus latitude, to analyze their relative position and deduce the possible role of the MLD in the supply of nitrates from the deep layers to the surface layers.

4 Results

4.1 Study area characterization

4.1.1 Sea surface temperature

The equatorial Atlantic region exhibits distinct, features such as the Atlantic cold tongue and coastal upwellings in the Gulf of Guinea and Angola during the first week of July. Analysis of SST variations in early June reveals a gradual warming trend along the African coastal regions, with temperatures ranging from 26.9 to 27.9°C. This warming trend gradually tapers southwards from Congo, reaching temperatures below 23°C. Notably, the equatorial region displays the characteristic cold tongue pattern, as confirmed by the temperature from June to August (Supplementary Figure S1). However, the area extending from southern Congo to Angola experiences anomalous warming with temperature anomalies of 2°C, concealed beneath the cold surface waters. This cooling effect is attributed to intensified surface mixing, possibly leading to the deepening of the MLD (D'Ortenzio et al., 2021).

4.1.2 Sea salinity

Vertical salinity structures between 2°N and 10°S at 10°W exhibit distinct seasonal patterns (Supplementary Figure S2). During June, the thermocline displays a convex structure, ascending to depths of 25 to 65 meters in the equatorial region, followed by a deepening trend between September and February to approximately 60 to 80 meters. In both seasons, deeper thermoclines ranging from 80 to 110 meters are observed in the subequatorial region. Surface waters exhibit higher salinity levels of 35 to 35.8 practical salinity units (PSU) during boreal summer, contrasting with the boreal winter period, where low salinity levels extend beyond 5°S. This is consistent with earlier studies by Hisard (1973), who also reported similar salinity values during the boreal summer. Subtropical salinity variations indicate an increase from 36 to 36.8 PSU around 10°S, with peaks in June at 10°S and other locations along the equator and subtropical regions (5°S and 5°S to 10°S). Indeed, the analysis of the E-P balance carried out by Michel (2006) presented strong positive correlations along the equator, which extended up to 10°S-10°W from December to September. Furthermore, in the GG, recent EGEE campaigns have shown the existence of barrier layer (BL) profiles with stratifications in the mixed layer at 10°S-10°W, confirmed by Wade et al. (2011). According to Peter (2007), this presence of BL is caused by the arrival from the subsurface of subtropical modal waters characterized by a maximum salinity.

4.1.3 Surface current

The South Equatorial Undercurrent (SEUC) spans the study area (Figure 2), with its core centered on 5 and 4°W, extending

vertically from 50 to 175 meters and exhibiting a strong eastward flow. The SEUC is a seasonal feature, prominent from January to June, gradually weakening in July and August. Its characteristics align with similar currents observed in the Pacific and Indian Oceans. The Average Directional Current Profiler (ADCP) measurements indicate modest average eastward velocities, reaching maximum values of 30 cm/s. In contrast, the South Equatorial Counter-current (SECC) displays relatively subdued surface velocities across the basin. Notably, the Equatorial Undercurrent (EUC) exhibits high velocities, reaching up to 50 cm/s, extending from the surface to 100 meters between 0°E and 1° E, facilitating the eastward transport of high-salinity waters (Napolitano et al., 2022).

4.1.4 Vertical nitrate distribution at 10°W

4.1.4.1 Boreal summer

The distribution of nitrate at 10°W in the GG during June and September reveals distinct patterns (Supplementary Figure S3). In the boreal summer (June), surface layers exhibit nitrate-rich content, with concentrations reaching 2 mmol m^{-3} in the upper 20 meters of the water column. Between 5°S and 10°S, nitrate levels of 0.5 mmol m^{-3} are observed at depths beyond 60 meters. In September, surface waters show increased nitrate levels, peaking at 2 mmol m^{-3} from 2°N to 5°S within the upper 40 meters. Nitrate concentrations of 0.5 mmol m^{-3} are present beyond 7°S.

4.1.4.2 Boreal winter

In the boreal winter, the meridional distribution of nitrate at 10° W in the GG (Supplementary Figure S3: November and February) closely resembles earlier observations (Voituriez et al., 1982; Oudot and Morin, 1987). Nitrate concentrations remain low within the upper 20 meters, registering below 0.5 mmol m^{-3} and decreasing further southward. Notably, isolines deepen at the equator while surfacing between 2°S and 5°S in November. An uplift of isolines between 2°S and 4°S indicates nitrate supply to the surface layers during both seasons.

4.1.5 Surface nitrate concentrations, nitracline top, and MLD

The results in Supplementary Table S1 emphasize the minimum, maximum, and mean values of the parameters studied.

In the equatorial region, during boreal winter, MLD ranges from 20.5 meters to 64.5 meters, with a mean of 39.06 meters. Nitracline top varies between 34.1 meters and 46.2 m, with a mean of 41.0 meters. Mean nitrate concentrations within the MLD are notably high, ranging from 2.96 mmol m^{-3} to 7.49 mmol m^{-3}, averaging 5.35 mmol m^{-3}. In boreal summer, MLD varies from 10.5 meters to 35.33 meters (mean: 25.88 meters), and nitracline fluctuates between 5.5 meters and 28.8 meters (mean: 14.68 meters). Nitrate concentration varies between 0 mmol m^{-3} and 2.06 mmol m^{-3}, with a mean of 1.6 mmol m^{-3}.

In this region, no significant difference was observed between the MLD values during the boreal summer and boreal winter (Student t-test, p = 0.226). On the other hand, a significant difference was obtained between the depths of the nitracline and between those of the nitrate concentration in the mixed layer with p-values of 0.001, lower than the significance value of 0.05 during both seasons. These results indicate that in the equatorial area, carrying out a seasonal study with the MLD is unnecessary. On the other hand, it is essential to opt for a seasonal study using the depth of the nitracline or the nitrate concentration in the mixed layer.

Subequatorial MLDs range from 30.93 meters to 44.13 meters (mean: 39.72 meters), nitracline top varies from 45.99 meters to 79.57 meters (mean: 60.77 meters), and mean nitrate concentrations within the MLD range from 0.03 mmol m^{-3} to 0.66 mmol m^{-3} (mean: 0.25 mmol m^{-3}). In the subtropical region, MLDs cluster around a mean of 46.15 meters (range: 10 - 65.33 meters), nitracline tops span from 0 to 113.38 meters, and mean nitrate concentrations within the MLD range from 0.25 mmol m^{-3} to 5.41 mmol m^{-3} (mean: 1.55 mmol m^{-3}).

During the boreal summer, the ANOVA (Peer-to-Peer Comparison of Dwass, Steel, Critchlow and Flingner: D SCF)

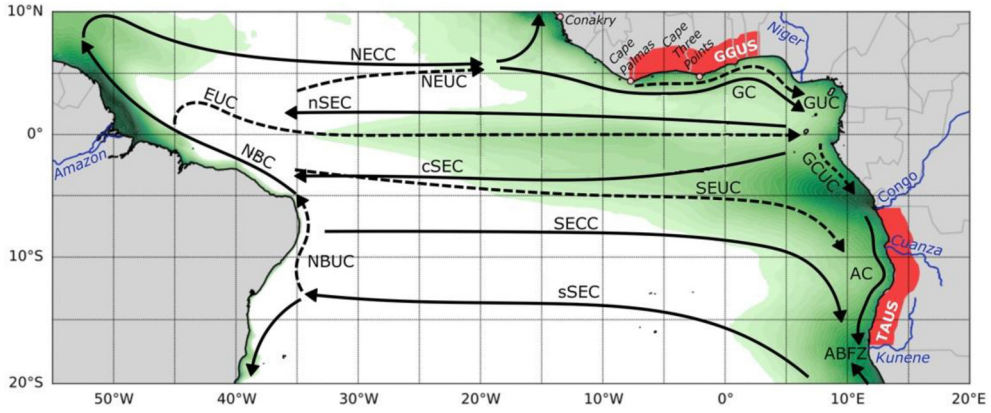

FIGURE 2
Map encompassing the surface and subsurface currents in the Gulf of Guinea. GC, Guinea Current; GUC, Guinea Undercurrent; SEUC, South Equatorial Undercurrent; EUC, Equatorial Undercurrent; nSEC, cSEC and sSEC, northern, central and southern branches of the South Equatorial Current (SEC) respectively; SECC, South Equatorial Countercurrent; GCUC, Gabon–Congo Undercurrent; AC, Angola Current. (Source: modified from Brandt et al., 2023, licensed CC-BY-4.0).

carried out for the three regions, between the MLDs, successively gave the following p-values: subequatorial-equatorial region 0.091; equatorial region-subtropical region 0.002 and subequatorial region-subtropical region 0.231. Only one significant test is noted between the equatorial and subtropical regions. A significant difference is then observed between the MLDs of the equatorial region and those of the subtropical region. On the other hand, there is no significant difference between the MLDs of the subequatorial-equatorial and subequatorial-subtropical regions.

The ANOVA (peer-to-peer comparison of DSCF) carried out for the three regions, between the depths of the nitracline, successively gave the following p-values: subequatorial-equatorial region 0.001; equatorial region-subtropical region 0.001 and subequatorial region-subtropical region 0.002. All the test were significant (p-values at 0.05). A significant difference is then observed between the depths of the nitracline of the three regions.

The ANOVA (peer-to-peer comparison of DSCF) carried out for the three regions, between the nitrate concentration levels, were significant for subequatorial-equatorial region (p-value at 0.001); equatorial region-subtropical region (p-value 0.001) and subequatorial region-subtropical region (p-value 0.015). A significant difference observed between the three regions' nitrate concentration levels as previously.

4.2 Spatial and seasonal average evolution of the MLD

The monthly vertical MLD distribution at 10°W reveals latitudinal variations (Figure 3). The equatorial region consistently shows the shallowest MLD, reaching 43 meters in October. Notably, the region south of the equator experiences MLD deepening from April to November, with maximum depths of 64.33 meters observed in May and November.

4.2.1 Boreal summer

During the boreal summer, the equatorial region demonstrates uniform MLD variation (Figure 4A). MLDs range from 10.5 to 35.33 meters at 1.5°N before gradually decreasing to 22 meters at 2° S. The nitracline remains above the mixed layer between 1.75°N and 2°S, while remaining below the MLD above 1.75°N. Nitracline depth ranges from 10.5 to 30 meters on average, decreasing from 2°S to 1°S (10 meters minimum) before deepening to 30 meters at 2° N. Nitrate concentration in the MLD ranges from near zero at 2°N to 2.06 mmol m^{-3} at 0.5°S, subsequently declining to 1.33 mmol m^{-3} at 2°S.

4.2.2 Subequatorial region

In the subequatorial region, MLD varies between 20 and 55 m (Figure 4B). It increases slightly from 40 m (6.75°S) to 55 m (5.75°S), then drops to 20 m at 5.5°S before deepening again to 35 m at 5.25°S. The nitracline consistently lies below the MLD, spanning approximately 50 to 90 m. It aligns closely with the MLD between 6°S and 5.25°S, deepening from 6°S to 6.75°S. Mean nitrate concentrations within the MLD remain low, below 0.5 mmol m^{-3}, except at 6°S, where concentrations of 0.66 mmol m^{-3} are observed.

4.2.3 Subtropical region

The subtropical region (8-10°S) displays distinctive hydrological characteristics (Figure 4C), with MLD ranging around a mean of 46.15 meters, from 10 to 65.33 meters. Nitracline top varies widely, from 0 to 113.38 meters, with a mean of 74.61 meters. Nitrate concentrations within the MLD range from 0.25 to 5.41 mmol m^{-3}, with the highest concentration of 5.41 mmol m^{-3} observed at 8°S. Notably, nitrate concentrations decrease sharply between 8.25°S and 8.75°S, remaining consistently below 0.25 mmol m^{-3} between 8.25°S and 9.75°S, except at 9°S, where concentrations reach 1.25 mmol m^{-3}.

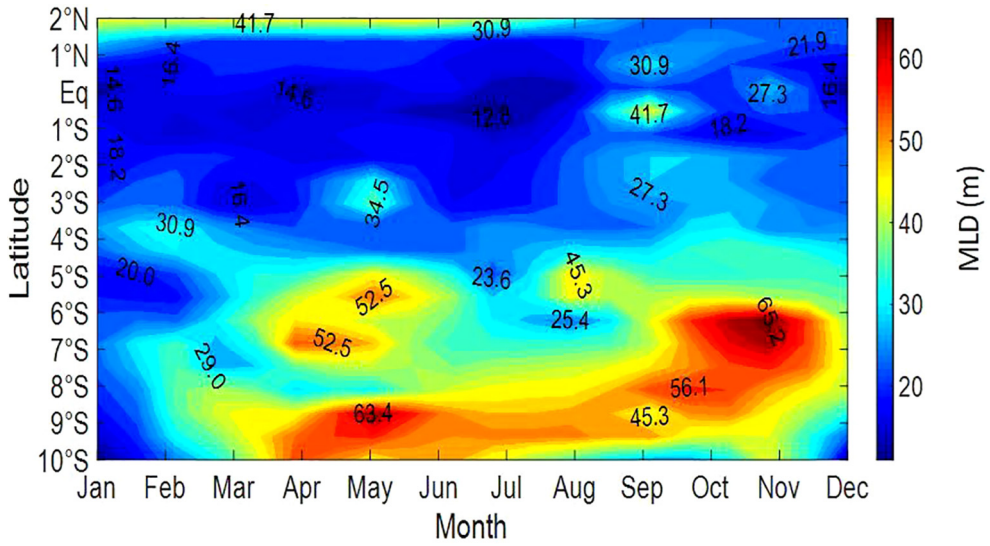

FIGURE 3
Hovmöller diagram of monthly mean Mixed Layer Depth 'MLD' (m) climatology based on density from 2°N to 10°S from 1973 to 2007 along the 10°W transect. Coded contours represent MLD.

The hydrological structure during boreal summer suggests that the nitracline's position influences nitrate input into the surface layers, with the equatorial region featuring nitracline within the mixed layer, and descending below the mixed layer as one moves southward from the equatorial region.

4.2.4 Boreal winter

The boreal winter demonstrates distinct MLD characteristics in the equatorial region (Supplementary Figure S4). The MLD thicknesses range from 20.5 to 64.5 meters, with the deepest points observed at 1°N and 1°S. The lowest MLD is recorded at 2°N (20.5 meters), while between 0.5°N and 0.5°S, the MLD is approximately 28.8 meters. The nitracline experiences minor variation, ranging between 42.12 and 44.14 meters. The nitracline depth decreases from 2°N to 1°N and from 0.5°S to 1°S, with minimum depths of 34.4 meters at 1°N and 34.4 meters at 1°S. An upward trend is observed from 1°N at the equator to 1°S, with a maximum depth of 46.19 meters. Nitrate concentrations within the MLD range from 3 to 7.49 mmol m^{-3}, with the highest concentrations observed at 1°N and 1°S. The boreal winter in the equatorial region demonstrates alternating positions of the nitracline and MLD, resulting in variable nitrate concentrations in the surface layer.

5 Discussion

The equatorial region experiences significant changes during the boreal summer. The Mixed Layer Depth (MLD) strengthens, reaching its seasonal maximum of 30 meters at 10°W, just south of the equator. This intensification is accompanied by lifting the nitracline top, a phenomenon reported by Voituriez et al. (1982) at 4°W. The rise in MLD leads to a notable input of nitrate into the surface layer, with concentrations ranging between 1.13 and 2.06 mmol m^{-3}. This finding is consistent with the results of other studies, such as those conducted by Cullen et al. (1983), Nubi et al. (2019), and Radenac et al. (2020), which also emphasize the contribution of nitrate to the ocean's surface layer during equatorial boreal summer.

Nubi et al. (2019) shed light on the role of equatorial upwelling in enriching nitrate concentrations, particularly evident at 10°W. This upwelling-driven nitrate enrichment is attributed to a weak pycnocline in the region. Hisard et al. (1977) and Monger et al.

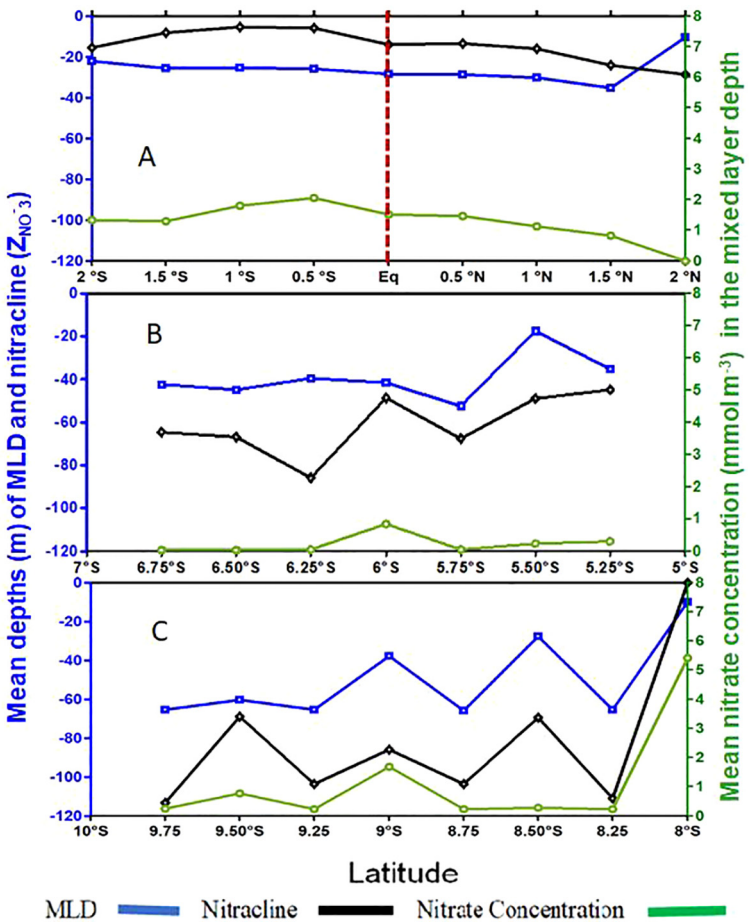

FIGURE 4
Spatial change of the mean Mixed Layer Depth 'MLD' (m), nitracline (m) and the mean nitrate concentration (mmol m^{-3}) in the mixed layer, during the boreal summer at 10°W. **(A)** Equatorial region, **(B)**: Subequatorial region, and **(C)** Subtropical region. The vertical red dashed line represents the Equator position.

(1997) further underscore the relationship between nitrate increases and the depth of the Equatorial Undercurrent (EUC) and nitracline. Radenac et al. (2001) extend the understanding by connecting elevated nitrate content to strengthened trade winds, resulting in conditions conducive to high organic production. A key observation is the association between increased nitrate concentrations and the deepening of the MLD south of the equator, as depicted in Figure 4A. This phenomenon is contrasted with the notion of nitrate increase being linked to the onset of upwelling, as Nubi et al. (2019) and Radenac et al. (2020) suggested. Radenac et al. (2001) provide further insight by demonstrating the influence of strengthened trade winds in supporting nitrate content growth through heightened organic production.

Radenac et al. (2001) establish a connection between nitrate content augmentation and intensified trade winds in equatorial Pacific waters, creating an environment conducive to high organic production. Similarly, Monger et al. (1997) propose upwelling as the driving force behind nitrate concentration escalation during boreal summer and early boreal winter. Grodsky et al. (2008) augment this explanation by highlighting the combined effect of equatorial upwelling and the shallowness of the nitracline. Remarkably, the boreal winter exhibits distinct dynamics in the equatorial region. During this period, the MLD attains its maximum depth, averaging 64.5 meters at 1°N and 1°S. This deepening of the MLD corresponds to elevated nitrate concentrations in the surface layer, with values peaking around 7.8 mmol m^{-3}. This increase commences at 2°N and 0.5°S, coinciding with the onset of MLD deepening. Notably, this finding contradicts the conclusions drawn by Herbland and Voituriez (1977, 1979), who suggest a nitrate-poor surface layer during boreal winter due to weak divergence. Instead, our study reveals a surface layer significantly enriched in nitrate under the influence of intensified MLDs. This contrasting observation underscores the complexity of equatorial oceanographic processes and the need for comprehensive understanding. Duffour and Stretta (1973) contribute to this understanding by showcasing strong nutrient enrichment, particularly nitrates, attributed to the divergence of the South Equatorial Current. This divergence triggers an upward movement of isolines, leading to enrichment at 1°N and 1°S. Notably, studies in the Gulf of Lion (Marty et al., 2002; de Fommervault, 2015) provide analogous evidence of high MLDs (reaching 425 meters) and by substantial nutrient content.

The dynamic between MLD and nutrient availability extends beyond equatorial regions. Investigations by Parard et al. (2014) reveal low nitrate concentrations within the subequatorial region (5° S-7°S), attributed to weak vertical advection inhibiting nitrate injection into the surface layer. However, a clear intake of nitrates is evident at 6° S, with concentrations reaching approximately 0.66 mmol m^{-3}. This enrichment is attributed to intense internal waves, which foster biological production and nutrient accumulation (Parard et al., 2014). Conversely, areas beyond 9°S exhibit increased MLD depths ranging from 60 to 70 meters, accompanied by diminished nitrate concentrations. These findings align with studies by Duffour and Stretta (1973), who observe quantitatively poor surface layers between 9°S and 12°S. This depletion is attributed to the low intensity of the south equatorial counter-current, preventing effective nutrient transport to the surface layer (Reid, 1964; Lemasson and Rebert, 1973).

Moreover, temperature and salinity variations contribute to the complex interplay of nutrient distribution and oceanographic processes. In-depth studies by Mayot (2016) highlight the role of reduced vertical mixing in decreasing primary production, resulting in lower nutrient concentrations in surface waters. This effect is exacerbated by saline waters carried by currents, which contribute to stratification and hinder nutrient influx into the surface layer (Niu et al., 2020; Dahunsi et al., 2023). These intricate interactions further emphasize the importance of the MLD in shaping nutrient availability and marine ecosystem dynamics. Atmospheric fluxes significantly influence MLD density changes and, consequently, nutrient distribution.

6 Conclusion

The equatorial region's oceanographic dynamics exhibit pronounced variations between boreal summer and winter. Boreal summers witness intensified upwelling and MLD strengthening, leading to enriched nitrate concentrations in the surface layer. This finding supports the role of equatorial upwelling and trade winds in enhancing nutrient availability and promoting organic production. Conversely, boreal winters highlight deepened MLDs and elevated nitrate concentrations in the equatorial region. This contradicts prior assumptions of nitrate-poor surface layers during this season, highlighting the influence of complex oceanographic processes.

Beyond the equatorial region, subequatorial zones experience diverse nitrate concentrations, driven by internal waves, advection, and current intensity. Temperature, salinity, and atmospheric fluxes shape nutrient distribution and primary production dynamics. These findings underscore the intricate relationships between oceanographic processes, nutrient availability, and marine ecosystem productivity. A comprehensive understanding of these interactions with the role of the Atlantic Equatorial biological pump is essential for informed resource management and the sustainability of fisheries in the Atlantic Equatorial region and beyond.

Data availability statement

The original contributions presented in the study are included in the article/Supplementary Materials. Further inquiries can be directed to the corresponding author.

Author contributions

KK: Conceptualization, Data curation, Formal analysis, Methodology, Software, Visualization, Writing – original draft, Writing – review & editing. KN: Data curation, Software, Visualization, Writing – original draft, Writing – review & editing. AK: Project administration, Supervision, Writing – original draft. AT: Project administration, Supervision, Writing – original draft. MO: Methodology, Writing – original draft. PB: Project administration, Visualization, Writing – original draft, Writing – review & editing.

Funding

The author(s) declare that financial support was received for the research, authorship, and/or publication of this article. This work was supported by the PREFACE project (Improving the prediction of the Atlantic tropical climate and its impacts; 2013-2017). This project has received funding from the European Union's Seventh Framework Programme for research; technological development and demonstration under grant agreement no 603521 and the AWA project (Ecosystem Approach to Fisheries Management and the Marine Environment in West African Waters; 2013-2018). This project has received funding from IRD (France) and BMBF (grant 01DG12073E), and implemented at CSRP/SRFC: Sub Regional Fisheries Commission.

Acknowledgments

We thank PIRATA (Prediction and Research Moored Array in the Tropical Atlantic) program, coordinated by UMR Legos associated with EAR Imago of IRD (France), for data collection. Special thanks to Pr Noël Kleenlyside (UiB, Norway) and Dr. Bernard Bourles (IRD, France) for early support.

Conflict of interest

The authors declare that the research was conducted in the absence of any commercial or financial relationships that could be construed as a potential conflict of interest.

Publisher's note

All claims expressed in this article are solely those of the authors and do not necessarily represent those of their affiliated organizations, or those of the publisher, the editors and the reviewers. Any product that may be evaluated in this article, or claim that may be made by its manufacturer, is not guaranteed or endorsed by the publisher.

Supplementary material

The Supplementary Material for this article can be found online at: https://www.frontiersin.org/articles/10.3389/fmars.2024.1198106/full#supplementary-material

SUPPLEMENTARY FIGURE 1
Climatology of seasonal sea surface temperature December–January-February (DJF); June–July-August (JJA). Data were from TropFlux (https://incois.gov.in/tropflux/index.jsp; accessed on 12 June 2019) (1979–2011). (Source: Cabos et al., 2019). The black dashed box indicates the study area (Gulf of Guinea).

SUPPLEMENTARY FIGURE 2
The latitudinal trend in monthly mean salinity (PSU) from 1973 to 2017 in the boreal summer (June and September) and boreal winter (November and February). The pink line represents the thermocline (m), and those in white are the isohalines. The vertical red dashed lines represent the Equator position.

SUPPLEMENTARY FIGURE 3
Mean vertical sections down to 100 m of nitrate concentrations (mmol m^{-3}) at 10°W from 1973 to 2007 in the boreal summer (June and September) and boreal winter (November and February). The white lines represent nitrate concentrations as a function of depth. Vertical blue dashed lines represent the Equator position.

SUPPLEMENTARY FIGURE 4
Spatial change of the mean mixed layer depth (MLD in m), nitracline and the mean nitrate concentration (mmol m^{-3}) in the Mixed Layer, during the boreal winter at 10°W in the equatorial region. The vertical red dashed line represents the Equator position.

SUPPLEMENTARY TABLE 1
Values of minimum, maximum, and mean of the Mixed Layer Depth "MLD" (m), nitracline depth (m), and mean of the NO_3^- concentrations (mmol m^{-3}) in the MLD during both seasons in the equatorial region and in the boreal summer for the subequatorial and subtropical areas at 10°W.

References

Aksnes, D. L., Ohman, M. D., and Rivière, P. (2007). Optical effect on the nitracline in a coastal upwelling area. *Limnol Oceanogr* 52, 1179–1187. doi: 10.4319/lo.2007.52.3.1179

Alvain, S. (2005). Etude de la distribution des principaux groupes de phytoplancton par télédétection satellitaire: développement de la méthode PHYSAT à partir des données GeP&CO et application à l'archive SEAWIFS entre 1998 et 2004. Université Paris-Diderot, Paris VII, France. Méthodes Physiques en Télédétection.

Bendschneider, K., and Robinson, R. J. (1952). A new spectrophotometric method for the determination of nitrite in water seawater. *J. Mar. Res. II* 11, 87–96. Available online at: https://elischolar.library.yale.edu/journal_of_marine_research/761

Bourlès, B., Brandt, P., Caniaux, G., Dengler, M., Gouriou, Y., Erica, C., et al. (2007). African monsoon multidisciplinary analysis (AMMA): special measurements in the tropical atlantic. *CLIVAR Exch* 12, 1–28.

Brandt, P., Alory, G., Awo, F. M., Dengler, M., Djakouré, S., Imbol Koungue, R. A., et al. (2023). Physical processes and biological productivity in the upwelling regions of the tropical Atlantic. *Ocean Sci.* 19 (3), 581–601. doi: 10.5194/os-19-581-2023

Brandt, P., Bordbar, M. H., Coelho, P., Koungue, R. A. I., Körner, M., Lamont, T., et al. (2024). "Physical drivers of southwest african coastal upwelling and its response to climate variability and change," in *Sustainability of Southern African Ecosystems under Global Change*. Eds. G. P. Von Maltitz, G. F. Midgley and J. Veitch (Springer International Publishing, Cham), pp 221–pp 257. doi: 10.1007/978-3-031-10948-5_9

Cabos, W., de la Vara, A., and Koseki, S. (2019). Tropical Atlantic variability: Observations and modeling. *Atmosphere* 10, 502. doi: 10.1357/002224083788520171

Cullen, J. J., Stewart, E., Renger, E., Eppley, R. W., and Winant, C. D (1983). Vertical motion of the thermocline, nitracline and chlorophyll maximum layers in relation to currents on the Southern California Shelf. *J Mar Res* 41, 239–262. doi: 10.1357/002224083788520171

D'Ortenzio, F., Lavigne, H., Besson, F., Claustre, H., Coppola, L., Garcia, N., et al. (2014). Observing mixed layer depth, nitrate and chlorophyll concentrations in the northwestern Mediterranean: A combined satellite and NO3 profiling floats experiment. *Geophys Res. Lett.* 41, 6443–6451. doi: 10.1002/2014GL061020

D'Ortenzio, F., Taillandier, V., Claustre, H., Coppola, L., Conan, P., Dumas, F., et al. (2021). BGC-argo floats observe nitrate injection and spring phytoplankton increase in the surface layer of levantine sea (Eastern Mediterranean). *Geophys Res. Lett.* 48, P. e2020GL091649 (11p.). doi: 10.1029/2020GL091649

Dahunsi, A. M., Oyikeke, T. S., Abdulfatai, M. A., and Afolabi, L. A. (2023). Spatio-temporal assessment of the impacts of the trends in physical and biogeochemical parameters on the primary production of the Gulf of Guinea. *Heliyon* 9, e13047. doi: 10.1016/j.heliyon.2023.e13047

de Fommervault, O.P. (2015). Dynamique des nutriments en Méditerranée: des campagnes océanographiques aux flotteurs Bio-Argo. Université Pierre et Marie Curie, Paris VI, France. Océan Atmosphère, Climat et Observations Spatiales.

Duffour, P., and Stretta, J.-M. (1973). Production primaire, biomasses du phytoplancton et du zooplancton dans l'Atlantique tropical sud, le long du méridien 4°W. *Cah ORSTOM Sér Océan* XI, 419–429.

Grodsky, S. A., Carton, J. A., and McClain, C. R. (2008). Variability of upwelling and chlorophyll in the equatorial Atlantic. *Geophys Res. Lett.* 35, 2007GL032466. doi: 10.1029/2007GL032466

Gruber, N., Keeling, C. D., and Bates, N. R. (2002). Interannual variability in the North Atlantic Ocean carbon sink. *Science* 298, 2374–2378. doi: 10.1126/science.1077077

Hales, B., Takahashi, T., and Bandstra, L. (2005). Atmospheric CO2 uptake by a coastal upwelling system. *Glob Biogeochem Cycles* 19 (1), GB1009. doi: 10.1029/2004GB002295

Hemsley, V. (2016). Primary production and nitrate budgets in the temperate North Atlantic estimated from ocean gliders. University of Southampton, United Kingdom. Ocean & Earth Science.

Herbland, A., Le Bouteiller, A., and Raimbault, P. (1985). Size structure of phytoplankton biomass in the equatorial Atlantic Ocean. *Deep Sea Res. Part Oceanogr Res. Pap* 32, 819–836. doi: 10.1016/0198-0149(85)90118-9

Herbland, A., and Voituriez, B. (1977). Evaluation de la production primaire et de la chlorophylle à partir des données hydrologiques: application au golfe de Guinée. *Doc. Sci. - CRO 1 Abidj* 8, 73–85.

Herbland, A., and Voituriez, B. (1979). Hydrological structure analysis for estimating the primary production in the tropical Atlantic Ocean. *J. Mar. Res.* 37, 87–101. Available online at: https://elischolar.library.yale.edu/journal_of_marine_research/1461.

Hisard, P. (1973). Variations saisonnières à l'équateur dans le Golfe de Guinée. *Cah ORSTOM Sér Océan* 11, 349–358.

Hisard, P., Citeau, J., and Voituriez, B. (1977). "Equatorial undercurrent influences on enrichment processes of upper waters in the Atlantic Ocean," in *Report of the International Workshop on the GATE Equatorial Experiment*(Miami), pp 1–pp10.

Holte, J., and Talley, L. (2009). A new algorithm for finding mixed layer depths with applications to argo data and subantarctic mode water formation. *J. Atmospheric Ocean Technol.* 26, 1920–1939. doi: 10.1175/2009JTECHO543.1

Hummels, R., Dengler, M., Brandt, P., and Schlundt, M. (2014). Diapycnal heat flux and mixed layer heat budget within the Atlantic Cold Tongue. *Clim Dyn* 43, 3179–3199. doi: 10.1007/s00382-014-2339-6

Ismail, K. A., and Al Shehhi, M. R. (2022). Upwelling and nutrient dynamics in the Arabian Gulf and sea of Oman. *PloS One* 17, e0276260. doi: 10.1371/journal.pone.0276260

Kolodziejczyk, N., Marin, F., Bourlès, B., Gouriou, Y., and Berger, H. (2014). Seasonal variability of the equatorial undercurrent termination and associated salinity maximum in the Gulf of Guinea. *Clim Dyn* 43, 3025–3046. doi: 10.1007/s00382-014-2107-7

Kouamé, K. D. (2022). Distribution de nitrates dans la couche de surface océanique en relation avec la variabilité spatiale et saisonnière de la profondeur de la couche de mélange en Atlantique Equatorial Est à 10°W. Université Félix Houphoët-Boigny (Abidjan, Côte d'Ivoire, Français. Chimie.

Lavigne, H., D'Ortenzio, F., Migon, C., Claustre, H., Testor, P., d'Alcalà, M. R., et al. (2013). Enhancing the comprehension of mixed layer depth control on the Mediterranean phytoplankton phenology: Mediterranean Phytoplankton Phenology. *J. Geophys Res. Oceans* 118, 3416–3430. doi: 10.1002/jgrc.20251

Le Bouteiller, A. (1986). Environmental control of nitrate and ammonium uptake by phytoplankton in the Equatorial Atlantic Ocean. *Mar. Ecol. Ser.* 30, 167–179. doi: 10.3354/meps030167

Lemasson, L., and Rebert, J.-P. (1973). Circulation dans le Golfe de Guinée: étude de la région d'origine du sous-courant ivoirien. *Cah ORSTOM Sér Océan* 11, 303–316.

Lévy, M., Ferrari, R., Franks, P. J. S., Martin, A. P., and Rivière, P. (2012). Bringing physics to life at the submesoscale: FRONTIER. *Geophys Res. Lett.* 39, 1–13. doi: 10.1029/2012GL052756

Mahadevan, A. (2016). The impact of submesoscale physics on primary productivity of plankton. *Annu. Rev. Mar. Sci.* 8, 161–184. doi: 10.1146/annurev-marine-010814-015912

Marty, J.-C., Chiavérini, J., Pizay, M.-D., and Avril, B. (2002). Seasonal and interannual dynamics of nutrients and phytoplankton pigments in the western Mediterranean Sea at the DYFAMED timeseries station, (1991–1999). *Deep Sea Res. Part II Top. Stud. Ocean* 49, 1965–1985. doi: 10.1016/S0967-0645(02)00022-X

Mayot, N. (2016). La saisonnalité du phytoplancton en Mer Méditerranée. Université Pierre et Marie Curie, Paris VI, France. Sciences de la Terre.

McGillicuddy, D. J. (2016). Mechanisms of physical-biological-biogeochemical interaction at the oceanic mesoscale. *Annu. Rev. Mar. Sci.* 8, 125–159. doi: 10.1146/annurev-marine-010814-015606

Michel, S. (2006). Télédétection de la salinité à la surface des océans: Variabilité de la salinité de surface d'après un modèle global de couche mélangée océanique. Université Paris VII – Denis Didero, France. Océanographie Physique et Spatiale.

Monger, B., McClain, C., and Murtugudde, R. (1997). Seasonal phytoplankton dynamics in the eastern tropical Atlantic. *J. Geophys Res.* 102, 12389–12411. doi: 10.1029/96JC03982

Morelle, J. (2017). Dynamique spatiale et temporelle de la production primaire de l'estuaire de la Seine. Université de Caen, Normandie. Physiologie et biologie des organismes - populations – interactions.

Murtugudde, R. G., Signorini, S. R., Christian, J. R., Busalacchi, A. J., McClain, C. R., and Picaut, J. (1999). Ocean color variability of the tropical Indo-Pacific basin observed by SeaWiFS during 1997-1998. *J. Geophys Res. Oceans* 104, 18351–18366. doi: 10.1029/1999JC900135

N'Guessan, B. K., Kouassi, A. M., Trokourey, A., Toualy, E., Kanga, D. K., and Brehmer, P. (2020). Eastern tropical Atlantic mixed layer depth: assessment of methods from *in situ* profiles in the gulf of Guinea from coastal to high sea. *Thalass Int. J. Mar. Sci.* 36, 201–212. doi: 10.1007/s41208-019-00179-7

Napolitano, D. C., Alory, G., Dadou, I., Morel, Y., Jouanno, J., and Morvan, G. (2022). Influence of the gulf of Guinea islands on the Atlantic equatorial undercurrent circulation. *J. Geophys Res. Oceans* 127, e2021JC017999. doi: 10.1029/2021JC017999

Niu, L., Van Gelder, P., Luo, X., Cai, H., Zhang, T., and Yang, Q. (2020). Implications of nutrient enrichment and related environmental impacts in the pearl river estuary, China: characterizing the seasonal influence of riverine input. *Water* 12, 3245. doi: 10.3390/w12113245

Nubi, O. A., Bourl Egrave, S. B., Edokpayi, C. A., and Hounkonnou, M. N. (2016). On the Nutrient distribution and phytoplankton biomass in the Gulf of Guinea equatorial band as inferred from *In-situ* measurements. *J. Oceanogr Mar. Sci.* 7, 1–11. doi: 10.5897/JOMS2016.0124

Nubi, O. A., Oyatola, O. O., and Bonou, F. (2019). Spatial variability in autumnal equatorial upwelling intensity within the Gulf of Guinea as inferred from in *situ* measurements. *J. Oceanogr Mar. Sci.* 10, 1–10. doi: 10.5897/JOMS2018.0146

Oudot, C. (1983). La distribution des sels nutritifs (NO3, - NO2, - NH4 - PO4, - Si03) dans l'Océan Atlantique intertropical oriental (région du Golfe de Guinée). *Océan Trop.* 18 (2), 223–248.

Oudot, C., and Morin, P. (1987). The distribution of nutrients in the Equatorial Atlantic: Relation to physical processes and phytoplankton biomass. *Oceanol Acta* (0399-1784), 121–130.

Parard, G., Boutin, J., Cuypers, Y., Bouruet-Aubertot, P., and Caniaux, G. (2014). On the physical and biogeochemical processes driving the high frequency variability of CO_2 fugacity at 6°S, 10°W: Potential role of the internal waves. *J. Geophys Res. Oceans* 119, 8357–8374. doi: 10.1002/2014JC009965

Pershing, A. (2006). BOOK REVIEW | Dynamics of marine ecosystems: biological-physical interactions in the oceans (Third edition). *Oceanography* 19, 157–159. doi: 10.5670/oceanog.2006.87

Peter, A.-C. (2007). Variabilité de la température de la couche de mélange océanique en Atlantique équatorial aux échelles saisonnières à interannuelles, à l'aide de simulations numériques. Université Paul Sabatier - Toulouse II, France. Océan, Atmosphère et Surfaces Continentales.

Radenac, M.-H., Jouanno, J., Tchamabi, C. C., Awo, M., Bourlès, B., and Arnault, S., et al. (2020). Physical drivers of the nitrate seasonal variability in the Atlantic cold tongue. *Biogeosciences* 17, 529–545. doi: 10.5194/bg-17-529-2020

Radenac, M. H., Menkes, C., Vialard, J., Moulin, C., Dandonneau, Y., Delcroix, T., et al. (2001). Modeled and observed impacts of the 1997–1998 El Niño on nitrate and new production in the equatorial Pacific. *J. Geophys Res. Oceans* 106, 26879–26898. doi: 10.1029/2000JC000546

Reid, J. L. (1964). A transequatorial Atlantic oceanographic section in July 1963 compared with other Atlantic and Pacific sections. *J. Geophys Res.* 69, 5205–5215. doi: 10.1029/JZ069i024p05205

Schafstall, J., Dengler, M., Brandt, P., and Bange, H. (2010). Tidal-induced mixing and diapycnal nutrient fluxes in the Mauritanian upwelling region. *J. Geophys Res. Oceans* 115, 2009JC005940. doi: 10.1029/2009JC005940

Sylla, A. (2019). Variabilité inter-annuelle à décennale et réponse aux forçages anthropiques de l'upwelling sénégalo-mauritanien. Sorbonne Université, Université Cheikh Anta Diop de Dakar, Sénégal. Océanographie.

Tréguer, P., and Le Corre, P. (1975). *Manuel d'Analyse Des Sels Nutritifs Dans L'eau de Mer (Utilisation de L'autoanalyzer II Technicon R). 2è èd* (Brest: UBO).

Trombetta, T. (2019). Initiation des efflorescences phytoplanctoniques en zone côtière: le rôle de la température et des interactions biologiques. Université Montpellier, France. Sciences agricoles.

Voituriez, B. (1983). Les variations saisonnières des courants équatoriaux à 4° W et l'upwelling équatorial du golfe de Guinée: 1. Le sous-courant équatorial. *Océan Trop.* 18, 163–183.

Voituriez, B., and Herbland, A. (1979). The use of the salinity maximum of the equatorial undercurrent for estimating nutrient enrichment and primary production in the Gulf of Guinea. *Deep Sea Res. Part Oceanogr Res. Pap* 26, 77–83. doi: 10.1016/0198-0149(79)90087-6

Voituriez, B., and Herbland, A. (1981). Primary production in the tropical Atlantic Ocean mapped from oxygen values of Equalant 1 and 2 (1963). *Bull. Mar. Sci.* 31, 853–863.

Voituriez, B., and Herbland, A. (1984). Signification de la relation nitrate/température dans l'upwelling équatorial du Golfe de Guinée. *Oceanol Acta* 7, 169–174.

Voituriez, B., Herbland, A., and Le Borgne, R. (1982). L'upwelling équatorial de l'Atlantique Est pendant l'Expérience Météorologique Mondiale (PEMG). *Oceanol Acta* 5, 301–314.

Wade, M., Caniaux, G., and du Penhoat, Y. (2011). Variability of the mixed layer heat budget in the eastern equatorial Atlantic during 2005–2007 as inferred using Argo floats. *J. Geophys Res.* 116, C08006. doi: 10.1029/2010JC006683

Williams, R. G., Roussenov, V., and Follows, M. J. (2006). Nutrient streams and their induction into the mixed layer. *Glob Biogeochem Cycles* 20, GB1016. doi: 10.1029/2005GB002586

Wilson, C., and Coles, V. J. (2005). Global climatological relationships between satellite biological and physical observations and upper ocean properties. *J. Geophys Res.* 110, C10001. doi: 10.1029/2004JC002724

Wood, E. D., Armstrong, F. A. J., and Richards, F. A. (1967). Determination of nitrate in seawater by cadmium-copper reduction to nitrite. *J. Mar. Biol. Assoc. UK* 47, 23–31. doi: 10.1017/S002531540003352X